EUROPEAN ORGANIZATION FOR NUCLEAR RESEARCH

A study of the decay width difference in the B_s^0–$\bar{B}_s^0$ system using $\phi\phi$ correlations

The ALEPH Collaboration[1]

Abstract

In a data sample of about four million hadronic Z decays recorded with the ALEPH detector from 1991 to 1995, the $B_s^0 \to D_s^{(*)+} D_s^{(*)-}$ decay is observed, based on tagging the final state with two ϕ mesons in the same hemisphere. The $D_s^{(*)+} D_s^{(*)-}$ final state is mostly CP even and corresponds to the short-lived B_s^0 mass eigenstate. The branching ratio of this decay is measured to be $\mathrm{BR}(B_s^0(\text{short}) \to D_s^{(*)+} D_s^{(*)-})$ = $(23 \pm 10\,{}^{+19}_{-9})\%$. A measurement of the lifetime of the $B_s^0(\text{short})$ gives $1.27 \pm 0.33 \pm 0.07$ ps. The lifetime and branching ratio measurements allow two essentially independent estimates to be made of the relative decay width difference $\Delta\Gamma/\Gamma$ in the $B_s^0 - \bar{B}_s^0$ system, corresponding to an average value $\Delta\Gamma/\Gamma = (25^{+21}_{-14})\%$.

---

[1]See the following pages for the list of authors.

The ALEPH Collaboration

R. Barate, D. Decamp, P. Ghez, C. Goy, J.-P. Lees, E. Merle, M.-N. Minard, B. Pietrzyk

Laboratoire de Physique des Particules (LAPP), IN[2]P[3]-CNRS, F-74019 Annecy-le-Vieux Cedex, France

R. Alemany, S. Bravo, M.P. Casado, M. Chmeissani, J.M. Crespo, E. Fernandez, M. Fernandez-Bosman, Ll. Garrido,[15] E. Graugés, M. Martinez, G. Merino, R. Miquel, Ll.M. Mir, A. Pacheco, H. Ruiz

Institut de Física d'Altes Energies, Universitat Autònoma de Barcelona, E-08193 Bellaterra (Barcelona), Spain[7]

A. Colaleo, D. Creanza, M. de Palma, G. Iaselli, G. Maggi, M. Maggi, S. Nuzzo, A. Ranieri, G. Raso, F. Ruggieri, G. Selvaggi, L. Silvestris, P. Tempesta, A. Tricomi,[3] G. Zito

Dipartimento di Fisica, INFN Sezione di Bari, I-70126 Bari, Italy

X. Huang, J. Lin, Q. Ouyang, T. Wang, Y. Xie, R. Xu, S. Xue, J. Zhang, L. Zhang, W. Zhao

Institute of High Energy Physics, Academia Sinica, Beijing, The People's Republic of China[8]

D. Abbaneo, G. Boix,[6] O. Buchmüller, M. Cattaneo, F. Cerutti, G. Dissertori, H. Drevermann, R.W. Forty, M. Frank, T.C. Greening, A.W. Halley, J.B. Hansen, J. Harvey, P. Janot, B. Jost, I. Lehraus, P. Mato, A. Minten, A. Moutoussi, F. Ranjard, L. Rolandi, D. Schlatter, M. Schmitt,[20] O. Schneider,[2] P. Spagnolo, W. Tejessy, F. Teubert, E. Tournefier, A.E. Wright

European Laboratory for Particle Physics (CERN), CH-1211 Geneva 23, Switzerland

Z. Ajaltouni, F. Badaud, G. Chazelle, O. Deschamps, A. Falvard, P. Gay, C. Guicheney, P. Henrard, J. Jousset, B. Michel, S. Monteil, J-C. Montret, D. Pallin, P. Perret, F. Podlyski

Laboratoire de Physique Corpusculaire, Université Blaise Pascal, IN[2]P[3]-CNRS, Clermont-Ferrand, F-63177 Aubière, France

J.D. Hansen, J.R. Hansen, P.H. Hansen,[1] B.S. Nilsson, A. Wäänänen

Niels Bohr Institute, DK-2100 Copenhagen, Denmark[9]

G. Daskalakis, A. Kyriakis, C. Markou, E. Simopoulou, A. Vayaki

Nuclear Research Center Demokritos (NRCD), GR-15310 Attiki, Greece

A. Blondel,[12] G. Bonneaud, J.-C. Brient, A. Rougé, M. Rumpf, M. Swynghedauw, M. Verderi, H. Videau

Laboratoire de Physique Nucléaire et des Hautes Energies, Ecole Polytechnique, IN[2]P[3]-CNRS, F-91128 Palaiseau Cedex, France

E. Focardi, G. Parrini, K. Zachariadou

Dipartimento di Fisica, Università di Firenze, INFN Sezione di Firenze, I-50125 Firenze, Italy

A. Antonelli, G. Bencivenni, G. Bologna,[4] F. Bossi, P. Campana, G. Capon, V. Chiarella, P. Laurelli, G. Mannocchi,[1,5] F. Murtas, G.P. Murtas, L. Passalacqua, M. Pepe-Altarelli

Laboratori Nazionali dell'INFN (LNF-INFN), I-00044 Frascati, Italy

J.G. Lynch, P. Negus, V. O'Shea, C. Raine, P. Teixeira-Dias, A.S. Thompson

Department of Physics and Astronomy, University of Glasgow, Glasgow G12 8QQ,United Kingdom[10]

R. Cavanaugh, S. Dhamotharan, C. Geweniger,[1] P. Hanke, G. Hansper, V. Hepp, E.E. Kluge, A. Putzer, J. Sommer, K. Tittel, S. Werner,[19] M. Wunsch[19]

Kirchhoff-Institut fï Physik, Universität Heidelberg, D-69120 Heidelberg, Germany[16]

R. Beuselinck, D.M. Binnie, W. Cameron, P.J. Dornan, M. Girone, N. Marinelli, J.K. Sedgbeer, J.C. Thompson,[14] E. Thomson[22]

Department of Physics, Imperial College, London SW7 2BZ, United Kingdom[10]

V.M. Ghete, P. Girtler, E. Kneringer, D. Kuhn, G. Rudolph

Institut für Experimentalphysik, Universität Innsbruck, A-6020 Innsbruck, Austria[18]

C.K. Bowdery, P.G. Buck, A.J. Finch, F. Foster, G. Hughes, R.W.L. Jones, N.A. Robertson

Department of Physics, University of Lancaster, Lancaster LA1 4YB, United Kingdom[10]

I. Giehl, K. Jakobs, K. Kleinknecht, G. Quast, B. Renk, E. Rohne, H.-G. Sander, H. Wachsmuth, C. Zeitnitz

Institut für Physik, Universität Mainz, D-55099 Mainz, Germany[16]

A. Bonissent, J. Carr, P. Coyle, O. Leroy, P. Payre, D. Rousseau, M. Talby

Centre de Physique des Particules, Université de la Méditerranée, IN^{2}P^3-CNRS, F-13288 Marseille, France

M. Aleppo, M. Antonelli, F. Ragusa

Dipartimento di Fisica, Università di Milano e INFN Sezione di Milano, I-20133 Milano, Italy

H. Dietl, G. Ganis, K. Hüttmann, G. Lütjens, C. Mannert, W. Männer, H.-G. Moser, S. Schael, R. Settles,[1] H. Stenzel, W. Wiedenmann, G. Wolf

Max-Planck-Institut für Physik, Werner-Heisenberg-Institut, D-80805 München, Germany[16]

P. Azzurri, J. Boucrot,[1] O. Callot, S. Chen, A. Cordier, M. Davier, L. Duflot, J.-F. Grivaz, Ph. Heusse, A. Jacholkowska,[1] F. Le Diberder, J. Lefrançois, A.-M. Lutz, M.-H. Schune, J.-J. Veillet, I. Videau,[1] D. Zerwas

Laboratoire de l'Accélérateur Linéaire, Université de Paris-Sud, IN^{2}P^3-CNRS, F-91898 Orsay Cedex, France

G. Bagliesi, T. Boccali, G. Calderini, V. Ciulli, L. Foà, A. Giassi, F. Ligabue, A. Messineo, F. Palla,[1] G. Rizzo, G. Sanguinetti, A. Sciabà, G. Sguazzoni, R. Tenchini,[1] A. Venturi, P.G. Verdini

Dipartimento di Fisica dell'Università, INFN Sezione di Pisa, e Scuola Normale Superiore, I-56010 Pisa, Italy

G.A. Blair, G. Cowan, M.G. Green, T. Medcalf, J.A. Strong

Department of Physics, Royal Holloway & Bedford New College, University of London, Surrey TW20 OEX, United Kingdom[10]

R.W. Clifft, T.R. Edgecock, P.R. Norton, I.R. Tomalin

Particle Physics Dept., Rutherford Appleton Laboratory, Chilton, Didcot, Oxon OX11 OQX, United Kingdom[10]

B. Bloch-Devaux, P. Colas, S. Emery, W. Kozanecki, E. Lançon, M.-C. Lemaire, E. Locci, P. Perez, J. Rander, J.-F. Renardy, A. Roussarie, J.-P. Schuller, J. Schwindling, A. Trabelsi,[21] B. Vallage

CEA, DAPNIA/Service de Physique des Particules, CE-Saclay, F-91191 Gif-sur-Yvette Cedex, France[17]

S.N. Black, J.H. Dann, R.P. Johnson, H.Y. Kim, N. Konstantinidis, A.M. Litke, M.A. McNeil, G. Taylor

Institute for Particle Physics, University of California at Santa Cruz, Santa Cruz, CA 95064, USA[13]

C.N. Booth, S. Cartwright, F. Combley, M. Lehto, L.F. Thompson

Department of Physics, University of Sheffield, Sheffield S3 7RH, United Kingdom[10]

K. Affholderbach, A. Böhrer, S. Brandt, C. Grupen, A. Misiejuk, G. Prange, U. Sieler

Fachbereich Physik, Universität Siegen, D-57068 Siegen, Germany[16]

G. Giannini, B. Gobbo

Dipartimento di Fisica, Università di Trieste e INFN Sezione di Trieste, I-34127 Trieste, Italy

J. Rothberg, S. Wasserbaech

Experimental Elementary Particle Physics, University of Washington, WA 98195 Seattle, U.S.A.

S.R. Armstrong, P. Elmer, D.P.S. Ferguson, Y. Gao, S. González, O.J. Hayes, H. Hu, S. Jin, J. Kile, P.A. McNamara III, J. Nielsen, W. Orejudos, Y.B. Pan, Y. Saadi, I.J. Scott, J. Walsh, J.H. von Wimmersperg-Toeller, Sau Lan Wu, X. Wu, G. Zobernig

Department of Physics, University of Wisconsin, Madison, WI 53706, USA[11]

1   Introduction

Mixing phenomena in neutral B meson systems provide an important test for Standard Model flavour dynamics. In the $B_s^0 - \bar{B}_s^0$ system, a direct measurement of the mass difference Δm_s between the mass eigenstates would yield precious information for the understanding of the quark mixing matrix parameters. Complementary insights can also be obtained from a measurement of the relative width difference $\Delta\Gamma/\Gamma$ between the B_s^0 mass eigenstates, expected to be the largest among b hadrons [1]. As $\Delta\Gamma$ and Δm_s are correlated, an experimental constraint on $\Delta\Gamma$ implies a corresponding constraint on the range of Δm_s.

Recent theoretical calculations predict a sizeable value of $\Delta\Gamma/\Gamma = 0.16 \pm 0.05$ in the $B_s^0 - \bar{B}_s^0$ system [2, 3] and motivate experimental efforts to measure this quantity. Neglecting the small correction from CP violation, the two CP eigenstates correspond to the short- and long-lived B_s^0 mass eigenstates. The CP even eigenstate is expected to decay more rapidly than the CP odd, as most of the decay products in the $b \to c\bar{c}s$ transition that are common to B_s^0 and $\bar{B}_s^0$ are CP even. Until now, investigations of $\Delta\Gamma/\Gamma$ have relied on isolating samples enriched in B_s mesons and attempting to measure the separate lifetimes of the CP eigenstates in the sample. For example, L3 [4] and CDF [5] have published constraints on $\Delta\Gamma/\Gamma$ based on double exponential fits to the proper time distributions of inclusive B and D_s-lepton samples respectively. The sensitivity of this approach is quadratic in $\Delta\Gamma/\Gamma$. Increased sensitivity to $\Delta\Gamma/\Gamma$ (first order in $\Delta\Gamma/\Gamma$) is achievable using samples enriched in only one CP eigenstate [1], although this method tends to suffer from a lack of statistics. Such an approach has been used by CDF [6] in the analysis of $B_s^0 \to J/\psi\ \phi$ decays.

This paper describes a study of the $B_s^0 \to D_s^{(*)+} D_s^{(*)-}$ decay, which is predominantly CP even [7], and is partially reconstructed in the $\phi\phi X$ final state [8]. The $\phi\phi$ vertex is used to reconstruct the B_s^0(short) decay length and eventually the proper time. From a fit to the proper time distribution it is possible to extract the lifetime of the B_s^0 candidates and an estimate of $\Delta\Gamma/\Gamma$. In addition, a new and essentially independent method for extracting $\Delta\Gamma/\Gamma$ using these events is introduced, based on a measurement of the branching ratio B_s^0(short) $\to D_s^{(*)+} D_s^{(*)-}$.

2   The ALEPH detector

The ALEPH detector and its performance are described in detail elsewhere [9, 10, 11]; only a brief description of the properties of the apparatus relevant for this analysis is given here. The subdetectors critical to this analysis are the tracking chambers, providing precise impact parameter measurement, decay length reconstruction, and particle identification (from dE/dx).

A high resolution vertex detector (VDET) consisting of two layers of double-sided silicon microstrip detectors surrounds the beam pipe. The inner layer is 6.5 cm from the beam

axis and covers 85% of the solid angle, and the outer layer is at an average radius of 11.3 cm and covers 69%. The spatial resolution for the $r\phi$ and z projections (transverse to and along the beam axis, respectively) is 12 μm at normal incidence. The vertex detector is surrounded by a drift chamber (ITC) with eight coaxial wire layers with an outer radius of 26 cm and by a time projection chamber (TPC) that measures up to 21 three-dimensional points per track at radii between 40 cm and 170 cm. These detectors are immersed in an axial magnetic field of 1.5 T and together measure the transverse momentum p_{T}, relative to the beam axis, of charged particles with a resolution $\sigma(p_{\mathrm{T}})/p_{\mathrm{T}} = 6 \times 10^{-4} p_{\mathrm{T}} \oplus 0.005$ (p_{T} in GeV/c). The resolution of the three-dimensional impact parameter in the transverse and longitudinal views for tracks having information from all tracking detectors and two VDET hits can be parametrized as $\sigma = 25\,\mu\mathrm{m} + 95\,\mu\mathrm{m}/p$ (p in GeV/c). The TPC also provides a measurement of the specific ionization energy loss of a charged track (dE/dx).

The selection of hadronic events is based on charged tracks and is described elsewhere [12]. The interaction point is reconstructed on an event-by-event basis using the constraint of the average beam spot position [11]. The resolution is 85 μm for $Z \to b\bar{b}$ events, projected along the sphericity axis of the event.

During 1998 the LEP1 data were reprocessed using a refined version of the reconstruction program. The main improvements concern the track reconstruction and the particle identification. A large number of changes were also made to the main helix-fitting routine. A new VDET pattern recognition algorithm allows groups of several nearby tracks which may share common hits to be analyzed together, to find the hit assignments that minimize the overall χ^2 for the event. The improvement in the hit association efficiency is more than 2% (from 89.2% to 91.0% in $r\phi$ and from 85.6% to 88.2% in z). Information on the drift time from the TPC wires is combined with that obtained from the pads to reduce the error in the z-coordinate by a factor of two. A 30% improvement in the $r\phi$ coordinate resolution is achieved for low transverse momentum tracks by correcting the pad coordinates for ionisation fluctuations along the tracks as measured by the wires. The particle identification (dE/dx) is improved by including pulse height data from the TPC pads with that of the wires, since the pad dE/dx is rarely saturated by high particle density in jets. This latter improvement is crucial for the present analysis because the dE/dx information is required for four charged tracks in each event.

3 Selection of B_s^0 double charm decays using $\phi\phi$ correlations

Candidates for the decay $B_s^0 \to D_s^{(*)+}D_s^{(*)-}$ are identified in hadronic Z events, where the two ϕ's from the $D_s \to \phi X$ decays are reconstructed in the same hemisphere with respect to the thrust axis. The ϕ candidates are reconstructed in the K^+K^- decay mode. Each kaon candidate must have a momentum greater than 1.5 GeV/c and a dE/dx measurement consistent with that expected for the kaon hypothesis and inconsistent with the pion
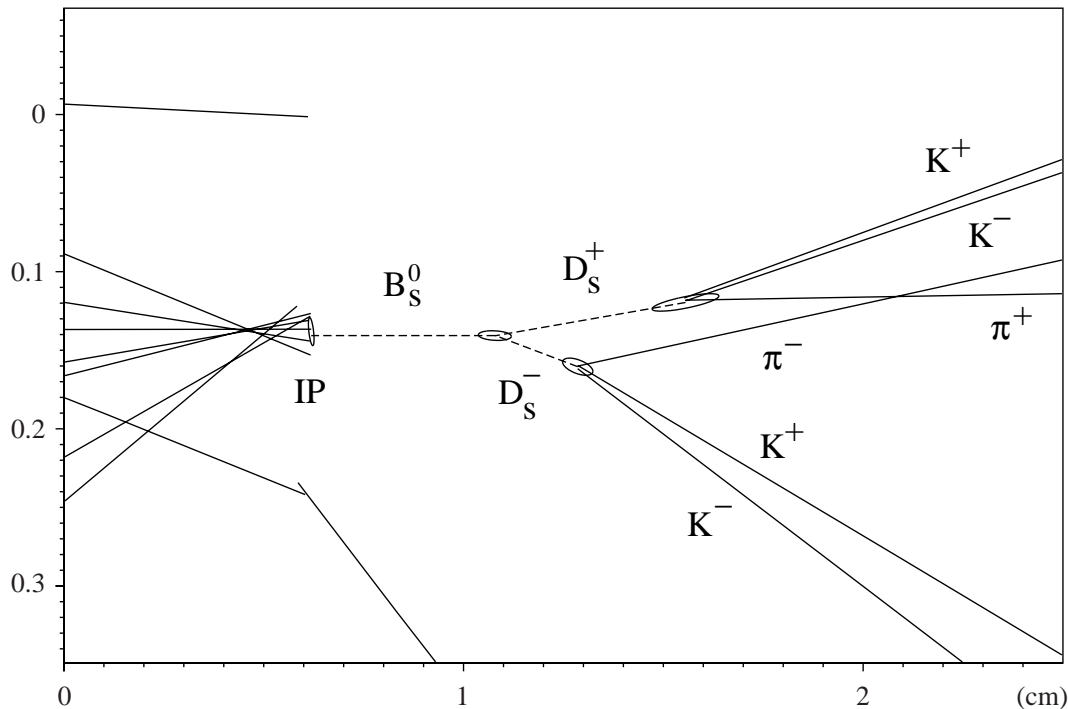
Figure 1: *Event display of a $B_s^0 \to D_s^{*+} D_s^{*-}$ candidate in the data, with two $D_s \to \phi\pi$ in the final state. The B_s^0 and D_s vertices are marked with their error ellipses and are well separated. The reconstructed invariant mass is compatible with the $B_s^0 \to D_s^{*+} D_s^{*-}$ hypothesis, with two missing photons from $D_s^* \to D_s\gamma$.*

hypothesis. To ensure good tracking quality, each kaon candidate must have at least one hit in the VDET.

To construct ϕ candidates, K^+K^- combinations are constrained to a common vertex, requiring the χ^2 probability of the vertex fit to be greater than 1%. Two ϕ candidates are then constrained to a common vertex, the $\phi\phi$ vertex, also demanding the χ^2 probability of the vertex fit to be greater than 1%. The $\phi\phi$ system must have a momentum greater than 10 GeV/c and an invariant mass between 2.75 and 4.5 GeV/c^2. The cosine of the decay angle of the most energetic ϕ in the $\phi\phi$ system, with respect to the $\phi\phi$ momentum, is required to be greater than -0.8. In Fig. 1 a particulary clean signal candidate is shown, with both D_s fully reconstructed in the $\phi\pi$ final state. The B_s^0 decay length $l_{B_s^0}$ is estimated by projecting the vector, in three dimensions, joining the interaction point and the $\phi\phi$ vertex onto the direction of flight of the $\phi\phi$ resultant momentum. For each event, the uncertainty $\sigma_{B_s^0}$ on the B_s^0 decay length is calculated from the track trajectory errors.

To reject the non-b events two alternative selection criteria are applied. For the branching ratio measurement a cut $l_{B_s^0}/\sigma_{B_s^0} > 2$ on the decay length of the B_s^0 is imposed. This cut is a good compromise between the efficiency and the purity of the sample but introduces a bias on the B_s^0 proper time distribution. The efficiency with the decay length
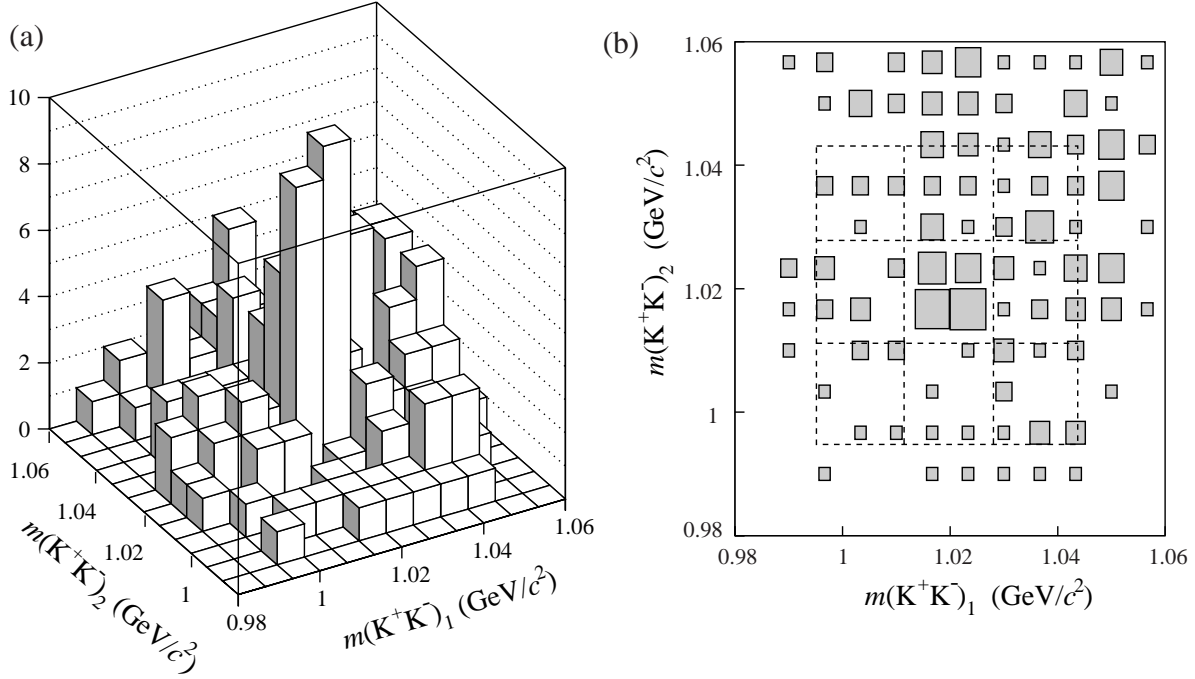
3

Figure 2: *Mass distribution of $m(K^+K^-)_1$ vs. $m(K^+K^-)_2$ for the events selected in the data: (a) displayed in perspective, (b) displayed as a box plot, where the area of each box is proportional to the bin contents; the regions used for event counting in Section 4 are indicated by the dashed lines.*

cut is about 9% with a b purity of 96% in the final sample.

For the lifetime measurement the proper time bias is avoided by replacing the cut on the decay length significance with a cut on the confidence level P_{uds} that the tracks in the hemisphere opposite to the $\phi\phi$ system originate from the primary vertex [13]. The cut $P_{uds} < 0.1$ is applied. The efficiency with this b tag requirement is 7% with a b purity of 93% in the final sample, slightly worse than that obtained with the decay length cut.

In Fig. 2 the $\phi\phi$ correlation in the data is plotted as a function of the mass of the two K^+K^- combinations for the lifetime based selection. A clear excess is observed in the region where the $\phi\phi$ signal is expected.

Besides the signal events $B_s^0 \to D_s^{(*)+}D_s^{(*)-}$, background processes can contribute to $\phi\phi$ combinations in hadronic Z decays. One or both ϕ's can originate from fragmentation or combinatorial background. This background component is strongly suppressed by the selection criteria. Four physics backgrounds are also present in $Z \to b\bar{b}$ and $Z \to c\bar{c}$ events:

1. $B_s \to D_s^{(*)-}D_s^{(*)+}X$, $D_s^- \to \phi X$, $D_s^+ \to \phi X$;

2. $B \to D_s^{(*)+}\bar{D}^{(*)}(X)$, $D_s^+ \to \phi X$, $\bar{D} \to \phi X$;

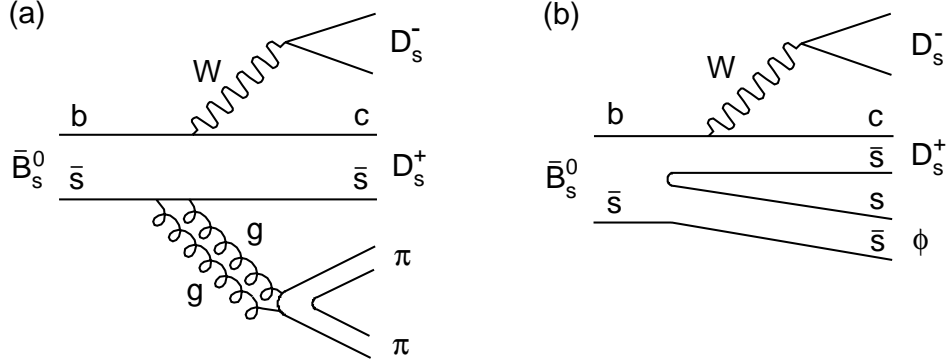3. $B_{(s)} \to D_{(s)}^{(*)}X$, $D_{(s)} \to \phi X$ and the second ϕ from fragmentation;

4

Figure 3: *Diagrams corresponding to the multi-body double charm decays of the B_s^0.*

4. $D_{(s)} \to \phi X$ and the second ϕ from fragmentation.

The first background component consists of the B_s^0 multi-body double charm decays that are not CP eigenstates and have not been observed experimentally. This component is strongly suppressed with respect to the signal, the two-body decay $B_s^0 \to D_s^{(*)+} D_s^{(*)-}$, for several reasons. Assuming a $\Delta I = 0$ rule for $b \to c\bar{c}s$ transitions [14], the decay to the $I = 1$ final state $B_s^0 \to D_s^{(*)+} D_s^{(*)-} \pi$ is forbidden, contrary to the situation for $B \to \bar{D}^{(*)} D_s^{(*)} \pi$ where the final state can have the same isospin value of the initial state $I = 1/2$. The allowed decay $B_s^0 \to D_s^+ D_s^- \pi\pi$ corresponding to the diagram plotted in Fig. 3(a) is suppressed by the need for two gluons, as in $\psi' \to J/\psi\ \pi\pi$. The $s\bar{s}$ popping in the B_s^0 decay of Fig. 3(b) is suppressed by kinematics because there would be at least a $D_s^+ D_s^- \phi$ in the final state, contrary to B^0 and B^+ equivalent decay diagrams with $q\bar{q}$ popping that have $\bar{D}D_s n\pi$ in the final state. Moreover these decays are almost all removed by the cut on $m_{\phi\phi} > 2.75$ GeV/c^2 and can therefore be neglected in this analysis.

For the second background component, the $D \to \phi X$ decay is Cabibbo and colour suppressed with respect to the signal process $D_s^+ \to \phi X$. It is important here to distinguish between the two-body $B \to \bar{D}^{(*)} D_s^{(*)+}$ and the multi-body decays. The multi-body background decays $B \to \bar{D}^{(*)} D_s^{(*)} n\pi$ have been measured by ALEPH to be more than half of these decays [15] and are suppressed by the cut on the invariant mass $m_{\phi\phi} > 2.75$ GeV/c^2. The two body $B \to DD_s, D^*D_s, DD_s^*, D^*D_s^*$ decays reproduce exactly the signal topology and cannot be removed by the selection. Their contribution can however be subtracted as their branching ratios are measured [15, 16, 17].

The last two background components are strongly suppressed by the requirements on the momenta, the mass, and the cosine of the decay angle in the $\phi\phi$ centre of mass system.

Fig. 4 shows the $\phi\phi$ invariant mass distribution after a ± 8 MeV/c^2 cut around the nominal ϕ mass is imposed for each $K^+ K^-$ combinations. The cut $m_{\phi\phi} > 2.75$ GeV/c^2 removes most of the combinatorial and physics backgrounds.
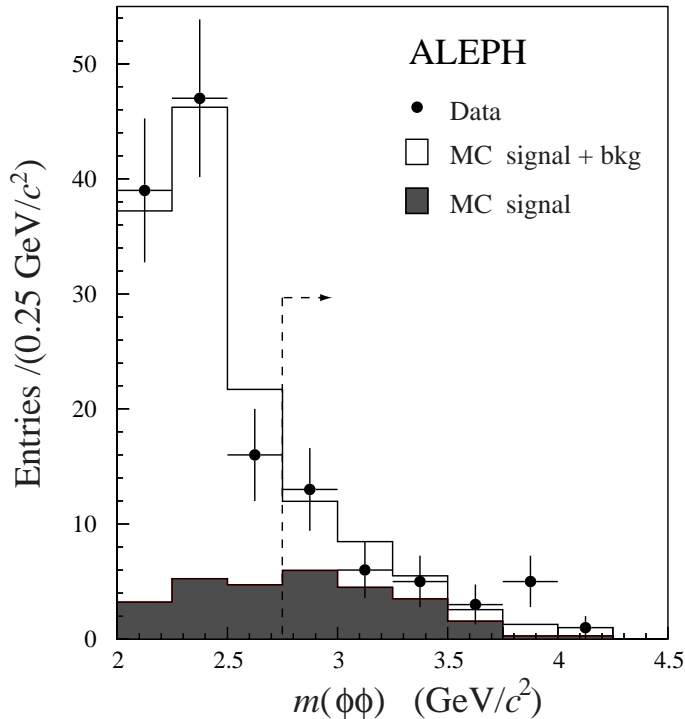
Figure 4: *Mass distribution of the $\phi\phi$ system before applying the cut $m_{\phi\phi} > 2.75 \ GeV/c^2$, which is indicated by the dashed line.*

4   Event counting

In order to evaluate the number of $\phi\phi$ events, the background must be subtracted, taking into account all the possible background combinations, the pure combinatorial component $(b_1 b_2)$ and the combinations of a true ϕ with a fake one $(\phi_1 b_2)$, $(b_1 \phi_2)$:

$$N_{\text{bkg}} = N(b_1 b_2) + N(b_1 \phi_2) + N(\phi_1 b_2) \ .$$

The number of background events is estimated from simple event counting averaged over symmetric sidebands around the $\phi\phi$ mass peak. In Fig. 5 the 9 regions defined to separate the signal region of each $K^+ K^-$ combination and the corresponding number of events found in the data are shown. All the numbers quoted in this section relate to the selection used for the branching ratio measurement, with the cut on decay length significance. For the lifetime measurement these numbers change a little, but the method used is the same. From Monte Carlo simulation the region where 98% of the signal is expected is found to be $\pm 8 \ \text{MeV}/c^2$ around the nominal mass of each ϕ. A width of 16 MeV$/c^2$ has been chosen for each box, in order to include all the signal events in the central box. The pure combinatorial background contribution $N(b_1 b_2)$ is estimated averaging the contents of the four bins belonging to the sidebands of the two ϕ's (i.e., the four corners of Fig. 5). The
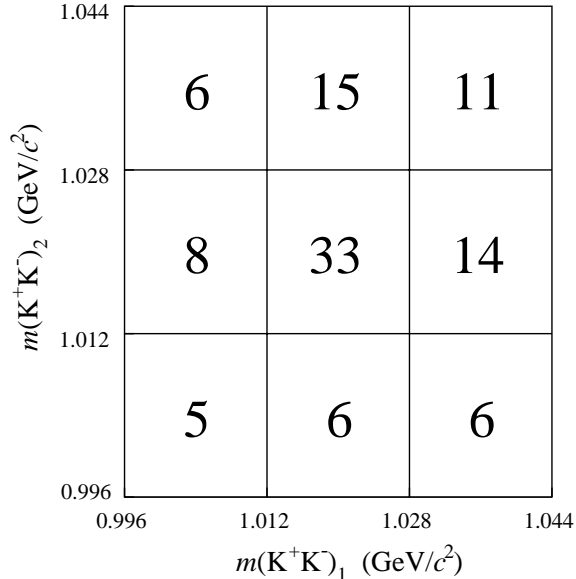
Figure 5: *Number of events selected in the data in the 9 regions of the plot of $m(K^+K^-)_1$ vs. $m(K^+K^-)_2$.*

contributions of $N(b_1\phi_2)$ and $N(\phi_1 b_2)$ are then computed in a similar way for events lying at the ϕ mass peak in one projection and in the ϕ sidebands in the other, after subtracting the pure combinatorial component of the background. The number of $\phi\phi$ events measured in this way is $N_{\phi\phi} = 18.5 \pm 6.7$. This method used to estimate the number of background events under the peak is exact when the background shape is linear. In the present case the background increases with the square root of the mass of each ϕ candidate, but the corrections due to this effect are found to be negligible.

For the final estimation of the number of $B_s^0 \to D_s^{(*)+}D_s^{(*)-}$ candidates, it is still necessary to subtract the contribution of $\phi\phi$ coming from B^0 and B^+ decays. The branching ratio of $B \to D_s^{+(*)}\bar{D}^{(*)}$ has been measured by ARGUS [16], CLEO [17] and ALEPH [15] and the current world average is $(4.9 \pm 1.3)\%$ [18]. The branching ratios for the inclusive decays of D^+ and D^0 to ϕ are obtained by summing the single branching ratio measurements of all the $D^+, D^0 \to \phi X$ decay modes [18] using the guidelines suggested in [19], giving $\mathrm{BR}(D^+ \to \phi X) = (1.1 \pm 0.2)\%$ and $\mathrm{BR}(D^0 \to \phi X) = (1.6 \pm 0.3)\%$. From these numbers, the physics background in the selected sample is estimated to be $N_{\mathrm{phy}}^{\mathrm{bkg}} = 3.7 \pm 1.1$ events. ALEPH has measured $\mathrm{BR}(B \to D_s^{(*)+}\bar{D}^{(*)}n\pi)$ to be $(9.4 \pm 5.0)\%$ [15], however the $\phi\phi$ mass cut used in the selection makes this background negligible, as it rejects 96% of such background events.

5 Measurement of the $B_s^0 \to D_s^{(*)+} D_s^{(*)-}$ branching ratio

The $B_s^0 \to D_s^{(*)+} D_s^{(*)-}$ branching ratio can be determined from the number of $\phi\phi$ signal events $N_{\phi\phi} - N_{\mathrm{phy}}^{\mathrm{bkg}}$, the total number of collected hadronic events $N_Z^{\mathrm{h}} = 4.2 \times 10^6$, the B_s fraction $f_s = (10.5 \pm 1.8)\%$ [18], the branching ratios of the $D_s^+ \to \phi X$ and the selection efficiency $\varepsilon = (9.5 \pm 0.5)\%$. Because only the short-lived component (CP even) of the B_s^0 decays to $D_s^{(*)+} D_s^{(*)-}$ (the CP odd component in this decay is estimated to be less than 2% of the CP even component [7]), it is more appropriate to quote the branching ratio of the short-lived B_s^0, using:

$$N_{\phi\phi} - N_{\mathrm{phy}}^{\mathrm{bkg}} = \varepsilon\, N_{B_s(\mathrm{short})}\, \mathrm{BR}(B_s^0(\mathrm{short}) \to D_s^{(*)+} D_s^{(*)-})\, \left[\mathrm{BR}(D_s^+ \to \phi X)\right]^2 \left[\mathrm{BR}(\phi \to K^+ K^-)\right]^2$$

where $N_{B_s(\mathrm{short})} = N_{B_s}/2 = N_Z^{\mathrm{h}} R_b f_s$ is the number of $B_s^0(\mathrm{short})$ produced. Using the measured fraction of hadronic Z decays into B hadrons, $R_b = 0.217 \pm 0.001$ [18] and the branching ratio $\mathrm{BR}(\phi \to K^+ K^-) = (49.1 \pm 0.6)\%$ [18], the following value is obtained:

$$\mathrm{BR}(B_s^0(\mathrm{short}) \to D_s^{(*)+} D_s^{(*)-}) = (23 \pm 10\ (\mathrm{stat}) \pm 5\ (\mathrm{syst}))\% \times \left[\frac{17\%}{\mathrm{BR}(D_s^+ \to \phi X)}\right]^2 .$$

The inclusive branching ratio of $D_s^+ \to \phi X$ has been factorized because it is the largest source of systematic uncertainty. The directly measured value of this branching ratio, $\mathrm{BR}(D_s^+ \to \phi X) = (18^{+15}_{-10})\%$ [20], is imprecise as it is measured with only three events. However, a better estimate can be obtained by summing the branching ratio of each measured exclusive mode [18]. In this way $\mathrm{BR}(D_s^+ \to \phi X) > (15.5 \pm 2.6)\%$ is found, where the lower limit reflects the fact that not all D_s^+ decays have yet been measured. Finally, it is possible to use the guidelines described in [19], summing all the measured $D_s^+ \to \phi X$ decay modes and estimating the others from isospin symmetry. Using this method, with the updated values of the exclusive D_s^+ branching ratios [18], $\mathrm{BR}(D_s^+ \to \phi X) = (4.72 \pm 0.46) \times \mathrm{BR}(D_s^+ \to \phi\pi)$ is obtained. With the measured $\mathrm{BR}(D_s^+ \to \phi\pi) = (3.6 \pm 0.9)\%$ [18] this gives:

$$\mathrm{BR}(D_s^+ \to \phi X) = (17.0 \pm 4.4)\% ,$$

which is consistent with (and more precise than) the directly measured value. This estimate is used, giving the final result:

$$\mathrm{BR}(B_s^0(\mathrm{short}) \to D_s^{(*)+} D_s^{(*)-}) = (23 \pm 10\ (\mathrm{stat})^{+19}_{-9}\ (\mathrm{syst}))\% .$$

The systematic uncertainties that affect the branching ratio measurement are listed in Table 1. The global uncertainty is dominated by the error $(^{+18\%}_{-8\%})$ that comes from the inclusive branching ratio $D_s^+ \to \phi X$. The systematic error due to the fraction f_s of B_s^0 in $Z \to b\bar{b}$ decays is 4%. In the Monte Carlo for the $B_s^0 \to D_s^{(*)+} D_s^{(*)-}$ decays

Table 1: *Sources of systematic uncertainty for the B_s^0(short) $\to D_s^{(*)+}D_s^{(*)-}$ branching ratio measurement.*

Source	Uncertainty
$BR(D_s^+ \to \phi X)$	$^{+18\%}_{-\ 8\%}$
B_s fraction f_s	$\pm 4\%$
Physics background	$\pm 2\%$
Monte Carlo branching fractions	$\pm 2\%$
Monte Carlo B_s^0 lifetime	$\pm 2\%$
Efficiency	$\pm 1\%$
dE/dx	$\pm 1\%$
Total	$^{+19\%}_{-\ 9\%}$

the relative fractions of $D_s^*D_s^*/D_s^*D_s/D_sD_s$ are arbitrary. The corresponding efficiencies of the $m_{\phi\phi}$ mass cut for these three modes are 54/65/75%. Considering an average mass cut efficiency of 65% and changing this value by 10%, it is possible to evaluate the corresponding systematic error (2%) on the branching ratio. The efficiency of the cut on the decay length significance is calculated assuming a B_s^0 lifetime of 1.49 ps. Using the B_s^0(short) lifetime obtained from the fit of the following section the efficiency changes by 7%, corresponding to a systematic uncertainty on the branching ratio of 2%. The systematic error due to the presence of the physics background, 2%, is calculated by varying the estimated number of these background events within their uncertainty. A systematic uncertainty of 1% reflects the statistical uncertainty on the selection efficiency. An error of 1% comes from the discrepancy between the data and the Monte Carlo on the efficiency of the dE/dx cut, which is evaluated using samples of kaons from D^{*+} decays and pions from K_S^0 decays.

6 Measurement of the B_s^0 proper time and lifetime fit

The B_s^0(short) lifetime is determined from the proper decay time distribution of the $\phi\phi$ events, after applying the opposite hemisphere b-tag requirement instead of the cut on the decay length significance, as described in Section 3. With this selection 16.2 ± 6.9 $\phi\phi$ events are found. For each B_s^0 candidate, the proper time is obtained from the decay length of the $\phi\phi$ system and the B_s^0 boost $\beta\gamma$:

$$t = \frac{l_{B_s^0}}{\beta\gamma} \ .$$

To estimate the precision on the decay length measurement, the difference between the measured and the true decay length is studied for Monte Carlo events. It is found that the $\phi\phi$ vertex is a reasonable unbiased approximation of the B_s^0 decay vertex, due to the short decay length of the D_s^+. The typical resolution of the B_s^0 decay length is 400 μm, compared with an average B_s^0 decay length of approximately 2.5 mm. To control the accuracy of the estimation of the event-by-event decay length uncertainty, the distribution of the difference between the measured and the true decay length, divided by its uncertainty, has been studied. The distribution is well parametrized by the sum of two centered Gaussian functions. The values of the parameters that define this resolution function, the two widths and the fractional area of the wider Gaussian, are found to be $\sigma_1 = 1.01 \pm 0.2$, $\sigma_2 = 3.0 \pm 0.3$ and $A_2 = 0.47$. This indicates that the uncertainty on the decay length is underestimated for about 50% of the events, corresponding to those in which the D_s^+ decay lengths are not negligible with respect to that of the B_s^0. A correction factor is applied to the measured decay length error to take this into account in the fit.

The B_s^0 boost is calculated with the nucleated jet method as the ratio between the momentum and the mass of the B_s^0 jet, reconstructed by adding charged and neutral objects to the $\phi\phi$ system using the technique described in [21]. Objects are clustered in the jet until the jet mass reaches 5.5 GeV/c^2 (optimized for the B_s^0). In order to take into account the uncertainty on the momentum reconstruction, a resolution function $K(k)$ is defined as the distribution of the ratio k of reconstructed to true momentum of the B_s^0 for Monte Carlo signal events. This distribution is parametrized with a Gaussian of mean value 1.01 ± 0.02 and width 0.12 ± 0.02.

The B_s^0(short) lifetime τ_S is extracted from an unbinned maximum likelihood fit to the proper time distribution of the B_s^0 candidates. The likelihood function contains a component for the $\phi\phi$ candidates in the peak (defined as 1.012 GeV/$c^2 < m(K^+K^-)_{1,2} <$ 1.028 GeV/c^2) and a component for events in the sidebands (defined as 0.98 GeV/$c^2 < m(K^+K^-)_{1,2} < 1.6$ GeV/c^2 after excluding the peak events). The latter are included to constrain the proper time parametrization of the combinatorial background in the peak region:

$$\mathcal{L} = \prod_i^{N_{\text{peak}}} [(1 - f_{\text{bkg}})\mathcal{P}_{\text{sig}}(t_i, \sigma_{t_i}, \tau_S) + f_{\text{bkg}}\mathcal{P}_{\text{bkg}}(t_i)] \times \prod_j^{N_{\text{side}}} \mathcal{P}_{\text{bkg}}(t_j) ,$$

where the coefficient f_{bkg} is the background fraction in the peak and $\mathcal{P}_{\text{sig}}(t, \sigma_t, \tau_S)$ is the probability function for the signal, consisting of an exponential function convolved with momentum and decay length resolution functions. The signal probability function also contains a fraction f_B of physics background $B \to D_s D$ parametrized with a second exponential with a lifetime constrained to an average of B^0 and B^+ lifetimes, $\tau_B = 1.6$ ps:

$$\mathcal{P}_{\text{sig}}(t, \sigma_t, \tau_S) = \left[(1 - f_B)\frac{e^{-t/\tau_S}}{\tau_S} + f_B \frac{e^{-t/\tau_B}}{\tau_B}\right] \otimes R(t, \sigma_1^l, \sigma_2^l) \otimes K(k) .$$

R is the decay length resolution function, parametrized with the sum of two Gaussians with widths $\sigma_{1(2)}^l = \sigma_{1(2)} \times \sigma_{B_s^0}$.

The function $\mathcal{P}_{\mathrm{bkg}}(t)$ is the normalized proper time distribution of the background, parametrized from the data. It consists of two components, a fraction f_0 of prompt (zero lifetime) background which is taken simply as a Gaussian resolution function of width σ_{bkg}, and a fraction of background having a lifetime τ_{bkg}, described by an exponential convolved with the same Gaussian resolution function:

$$\mathcal{P}_{\mathrm{bkg}}(t) = f_0 \; G(t, \sigma_{\mathrm{bkg}}) \; + \; (1 - f_0) \; \frac{e^{-t/\tau_{\mathrm{bkg}}}}{\tau_{\mathrm{bkg}}} \otimes G(t, \sigma_{\mathrm{bkg}}) \; .$$

In the fit there are three free parameters: the two lifetimes τ_{S}, τ_{bkg} and the fraction f_0. Figure 6 shows the result of the fit to the signal and background events. The fitted $B_s^0(\mathrm{short})$ lifetime is $\tau_{\mathrm{S}} = 1.27 \pm 0.33$ ps where the quoted uncertainty is statistical only.

Several sources of systematic uncertainty affecting this measurement have been investigated, and their respective contributions are summarized in Table 2. The systematic effects due to the fraction and the shape of the combinatorial background are included in the statistical error as the lifetime fit gives simultaneously the background parameters. The other systematic uncertainties come from the momentum and decay length resolutions and from the parameters describing the physics background. They are calculated by varying within their uncertainties the parametrization of the resolution function and the fraction and the time distribution for the physics background events. The total systematic error is, however, small compared to the statistical uncertainty:

$$\tau_{\mathrm{S}} = 1.27 \pm 0.33 \; (\mathrm{stat}) \pm 0.07 \; (\mathrm{syst}) \; \mathrm{ps} \; .$$

7 The evaluation of $\Delta\Gamma/\Gamma$

If the two B_s^0 eigenstates (short- and long-lived) have decay widths $\Gamma_{\mathrm{S,L}} = 1/\tau_{\mathrm{S,L}}$, it is possible to define the average width as $\Gamma = (\Gamma_{\mathrm{S}} + \Gamma_{\mathrm{L}})/2$ and the width difference $\Delta\Gamma = \Gamma_{\mathrm{S}} - \Gamma_{\mathrm{L}}$. There are two essentially independent evaluations of $\Delta\Gamma/\Gamma$ in this analysis. The first is based on the branching ratio measurement of the decay $B_s^0(\mathrm{short}) \to D_s^{(*)+} D_s^{(*)-}$. The second combines the measurement of the short-lived lifetime with the world average B_s^0 lifetime from semileptonic decays.

7.1 $\Delta\Gamma/\Gamma$ from the branching ratio

An estimate of $\Delta\Gamma/\Gamma$ can be obtained from the branching ratio measurement, under the assumption that the width difference between the two states is entirely due to the $B_s^0 \to D_s^{(*)+} D_s^{(*)-}$ decay, which is CP even. This hypothesis relies on the assumption that only decays to CP eigenstates can contribute to the width difference. Thus, in addition to the $B_s^0 \to D_s^{(*)+} D_s^{(*)-}$ decay, other decays such as $B_s^0 \to J/\psi \; \phi, \eta_c \eta, \psi^{'} \phi, J/\psi \; \eta$, etc. can also contribute in principle, however these decays are rare, and their contribution to $\Delta\Gamma/\Gamma$ is expected to be less than 5% of that expected for the $D_s^{(*)+} D_s^{(*)-}$ decays [7].
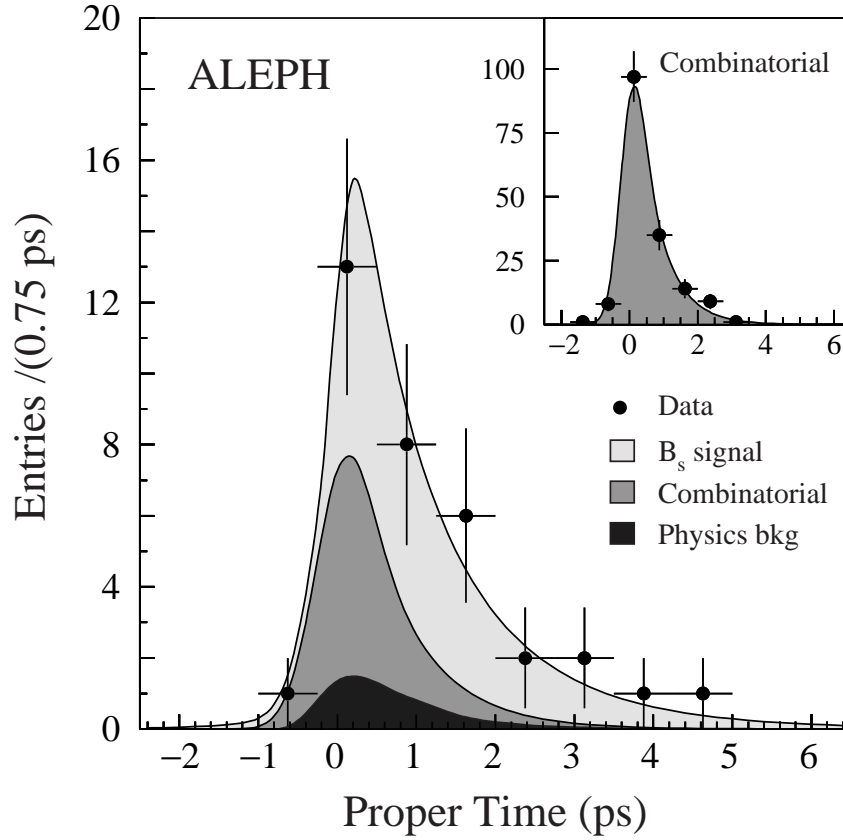
Figure 6: *The proper-time distribution of the B_s^0 candidates in the $\phi\phi$ sample. The dark shaded areas correspond to the proper time distributions of the combinatorial and physics backgrounds. The solid line is the result of the maximum likelihood fit. The inset shows the proper time distribution of the combinatorial background from the sidebands with the fitted parametrization.*

Table 2: *Sources of systematic uncertainty in the B_s^0 lifetime measurement.*

Source	Uncertainty (ps)
Resolution function	± 0.05
Momentum reconstruction	± 0.04
Physics background	± 0.02
Total	± 0.07

The other three- or four-body decays that have a CP defined final state are not pure CP even eigenstates, but can be CP odd or CP even depending on the angular momentum. Therefore the contribution of all these modes to $\Delta\Gamma/\Gamma$ is expected to be negligible compared to $\Gamma(B_s^0 \to D_s^{(*)+}D_s^{(*)-})$. With this assumption,

$$\Delta\Gamma = [\Gamma(\text{CP} = \text{even}) - \Gamma(\text{CP} = \text{odd})] = \Gamma(B_s^0(\text{short}) \to D_s^{(*)+}D_s^{(*)-})$$

and $\Delta\Gamma/\Gamma$ is related to the branching ratio of the decay $B_s^0(\text{short}) \to D_s^{(*)+}D_s^{(*)-}$ through

$$\text{BR}(B_s^0(\text{short}) \to D_s^{(*)+}D_s^{(*)-}) = \frac{\Gamma(B_s^0(\text{short}) \to D_s^{(*)+}D_s^{(*)-})}{\Gamma_{\text{S}}} = \frac{\Delta\Gamma}{\Gamma_{\text{S}}} = \frac{\Delta\Gamma}{\Gamma(1 + \Delta\Gamma/2\Gamma)} \ .$$

The measurement described above yields

$$\Delta\Gamma/\Gamma = (26^{+30}_{-15})\% \ ,$$

where the error is mostly systematic and is due to the uncertainty on the $D_s^+ \to \phi X$ branching ratio.

7.2 $\Delta\Gamma/\Gamma$ from the lifetime measurement

From the lifetime measurement of the CP even eigenstate, it is possible to extract $\Delta\Gamma/\Gamma$ from comparison with the average semileptonic B_s^0 lifetime. When an experiment measures a lifetime using a single exponential fit to the observed proper time distribution, the fitted lifetime is biased to the long lifetime component in the sample [22]. If the B_s^0 events are selected through the semileptonic decays $B_s^0 \to D_s^+ l^- \bar{\nu}$, the measured value from a fit with a single exponential is [22]

$$\tau_{\text{sl}} = (1/\Gamma) \frac{1 + (\frac{\Delta\Gamma}{2\Gamma})^2}{1 - (\frac{\Delta\Gamma}{2\Gamma})^2} \ .$$

With this formula $\Delta\Gamma/\Gamma$ can be expressed as a function of the lifetime of the short component τ_{S} and the semileptonic average τ_{sl}:

$$\frac{\Delta\Gamma}{\Gamma} = 2 \left[1 - \frac{\tau_{\text{S}}}{\tau_{\text{sl}}} \left(1 + (\tfrac{\Delta\Gamma}{2\Gamma})^2 \right) \right] \ .$$

As expected $\Delta\Gamma/\Gamma$ is almost linear in τ_{S}, with a small quadratic correction. With the present measurement $\tau_{\text{S}} = 1.27 \pm 0.34$ ps and the average of the B_s^0 lifetime measured in the semileptonic decays $\tau_{\text{sl}} = 1.45 \pm 0.06$ ps [23], the following result is obtained:

$$\Delta\Gamma/\Gamma = (22^{+38}_{-51})\% \ ,$$

where the statistical and systematic uncertainties are combined.

7.3 Average

In order to combine the two measurements, the result of each analysis, including the systematic error, is converted to a log-likelihood of $\Delta\Gamma/\Gamma$. The two measurements are basically independent. The only possible correlation between the two estimates is in the treatment of the systematic uncertainty on the branching ratio due to B_s^0(short) lifetime, and on the sytematic errors due to the physics background fraction. However, compared with the total uncertainty, these errors are negligible and therefore the two measurements are essentially uncorrelated.

From the sum of the two log-likelihoods the average value is estimated with its uncertainty:

$$\Delta\Gamma/\Gamma = (25^{+21}_{-14})\% \ .$$

The ratio $\Delta\Gamma/\Delta m_s$ is given by $\frac{3}{2}\pi m_b^2/m_t^2$ to first approximation, and when computed to next-to-leading order [2], adding the recent lattice calculation [3], is found to be $\Delta\Gamma/\Delta m_s = 6.5 \times 10^{-3}$ [24], with a preliminary estimate of the uncertainty of $\pm 30\%$. Using this value the corresponding value for the mass difference is $\Delta m_s = 26^{+22}_{-16}$ ps^{-1}.

8 Conclusion

In a total of about 4 million hadronic Z decays collected with the ALEPH detector between 1991 and 1995, the events with two ϕ mesons in the same hemisphere are studied. A clear enhancement in the number of events is observed, corresponding to $\phi\phi$ production. This excess of events is attributed primarily to the B_s^0 decay to the mostly CP even eigenstate $D_s^{(*)+}D_s^{(*)-}$ that corresponds to the short-lived mass state.

The branching ratio for this decay is measured to be $\mathrm{BR}(B_s^0(\text{short}) \to D_s^{(*)+}D_s^{(*)-}) = (23 \pm 10 \ (\text{stat}) \pm 5 \ (\text{syst}))\% \times \left[\frac{17\%}{\mathrm{BR}(D_s^+ \to \phi X)}\right]^2$. Using $\mathrm{BR}(D_s^+ \to \phi X) = (17.0 \pm 4.4)\%$ this corresponds to:

$$\mathrm{BR}(B_s^0(\text{short}) \to D_s^{(*)+}D_s^{(*)-}) = (23 \pm 10 \ (\text{stat})\,^{+19}_{-9} \ (\text{syst}))\% \ .$$

A maximum likelihood fit to the proper time distribution of the selected $B_s^0 \to D_s^{(*)+}D_s^{(*)-}$ candidates yields an estimate of the lifetime of the short-lived component:

$$\tau_{\mathrm{S}} = 1.27 \pm 0.33 \ (\text{stat}) \pm 0.07 \ (\text{syst}) \ \text{ps} \ .$$

Both these measurements enable essentially independent estimates of $\Delta\Gamma/\Gamma$ for the $B_s^0 - \bar{B}_s^0$ system to be obtained. Combining these yield the average:

$$\Delta\Gamma/\Gamma = (25^{+21}_{-14})\% \ .$$

Acknowledgements

References

[1] M.B. Voloshin *et al.*, *"On inclusive hadronic widths of beautiful particles"*, Yad. Fiz. **46** (1987) 181.

[2] M. Beneke *et al.*, *"Next-to-leading order QCD corrections to the lifetime difference of B_s^0 mesons"*, Phys. Lett. **B 459** (1999) 631.

[3] S. Hashimoto, *"B decays on the lattice"*, hep-lat/9909136, KEK–CP–093 (October 1999).

[4] The L3 Collaboration, *"Upper limit on the lifetime difference of short- and long-lived B_s^0 mesons"*, Phys. Lett. **B 438** (1998) 417.

[5] The CDF Collaboration, *"Measurement of the B_s^0 meson lifetime using semileptonic decays"*, Phys. Rev. **D 59** (1999) 032004.

[6] The CDF Collaboration, *Measurement of B hadron lifetimes using J/ψ final states at CDF*, Phys. Rev. **D 57** (1998) 5382.

[7] R. Aleksan *et al.*, *"Estimation of $\Delta\Gamma$ for the $B_s^0 - \bar{B}_s^0$ system. Exclusive decays and the parton model"*, Phys. Lett. **B 316** (1993) 567.

[8] I. Dunietz, *"$B_s^0 - \bar{B}_s^0$ mixing, CP violation, and extraction of CKM phases from untagged B_s^0 data samples"*, Phys. Rev. **D 52** (1995) 3048.

[9] The ALEPH Collaboration, *"ALEPH: a detector electron-positron annihilations at LEP"*, Nucl. Instrum. Methods **A 294** (1990) 121.

[10] B. Mours *et al.*, *"The design, construction and performance of the ALEPH silicon vertex detector"*, Nucl. Instrum. Methods **A 379** (1996) 101.

[11] The ALEPH Collaboration, *"Performance of the ALEPH detector at LEP"*, Nucl. Instrum. Methods **A 360** (1995) 481.

[12] The ALEPH Collaboration, *"Measurement of the Z Resonance Parameters at LEP"*, CERN EP/99-104.

[13] The ALEPH Collaboration, *"A precise measurement of* $\Gamma_{Z \to b\bar{b}} / \Gamma_{Z \to b\bar{b}}$ *"*,
Phys. Lett. **B 313** (1993) 535.

[14] M.J. Lipkin and A.I. Sanda, *"Isospin invariance, CP violation and* $B^0 - \bar{B}^0$ *mixing"*,
Phys. Lett. **B 201** (1988) 541.

[15] The ALEPH Collaboration, *"Observation of doubly-charmed B decays at LEP"*,
Eur. Phys. J **C 4** (1998) 387.

[16] The ARGUS Collaboration, *"Production of* $D^+_{(s)}$ *mesons in B decays and
determination of* $f(D_{(s)})$*"*, Z. Phys. **C 54** (1992) 1.

[17] The CLEO Collaboration, *"Measurements of* $B \to D_s X$ *decays"*,
Phys. Rev. **D 53** (1996) 4734.

[18] C. Caso *et al.*, Particle Data Group, Eur. Phys. J **C 3** (1998) 1.

[19] P. Roudeau and A. Stocchi, *"Inclusive branching fractions of* D^0*,* D^+*,* D_s *into* ϕ
mesons", LAL 93–03 (September 1993).

[20] The BEPC-BES Collaboration, *"Direct measurement of* $B(D^+_s \to \phi X^+)$*"*,
Phys. Rev. **D 57** (1998) 28.

[21] The ALEPH Collaboration, *"Measurement of mean lifetime and branching fractions
of b hadrons decaying to* J/ψ*"*, Phys. Lett. **B 295** (1992) 396.

[22] K. Hartkorn and H.-G. Moser, *"A new method of measuring* $\Delta\Gamma/\Gamma$ *in the* $B^0_s - \bar{B}^0_s$
system", Eur. Phys. J **C 8** (1999) 381.

[23] P. Coyle, *"B hadron lifetimes and* $\Delta\Gamma_s$*"*, to appear in the proceedings of the Int.
Europhys. Conf. on High Energy Physics, Tampere, Finland, 15–21 July 1999.

[24] M. Beneke, private communication, updating [2] with the recent lattice calculations
of [3].